

Assessment of Landsat 8 TIRS data capability for the preliminary study of geothermal energy resources in West Sumatra

Yuhendra¹, Joshapat Tetuko Sri Sumantyo²

¹Department of Informatics, Faculty of Engineering, Padang Institute of Technology, Indonesia

²Joshapat Microwave Remote Sensing, Chiba University, Japan

Article Info

Article history:

Received Mar 27, 2020

Revised Apr 23, 2020

Accepted May 1, 2020

Keywords:

DEM SRTM

Geothermal energy

Landsat-8 TIRS

LST

Remote sensing

West Sumatra

ABSTRACT

West Sumatra is one of has big geothermal energy resources potential. Remote sensing technology can have a role in geothermal exploration activity to measure the distribution of land surface temperatures (LST) and predict the geothermal potential area. Main study to obtain the assessment of Landsat 8 TIRS (Landsat's Thermal Infrared Sensor) data capability for geothermal energy resources estimation. Mono-window algorithms were used to generate the LST maps. Data set was combined with a digital elevation model (DEM) to identify the potential geothermal energy based on the variation in surface temperature. The result that were derived from LST map of West Sumatra shows that ranged from -8.6 C^0 to 32.59 C^0 and the different temperatures are represented by a graduated pink to brown shading. A calculated result clearly identifies the hot areas in the dataset, which are brown in colour images. Lima Puluh Kota, Tanah Datar, Solok, and South Solok areas showed the high-temperature value (Brown) in the range of 28.1 C^0 to 32.59 C^0 color in images which means that they possess high potential for generating thermal energy. In contrast, the temperatures were lower (Pink) in the north-eastern areas and the range distribution was from -8.5 C^0 to 5 C^0 .

This is an open access article under the [CC BY-SA](https://creativecommons.org/licenses/by-sa/4.0/) license.



Corresponding Author:

Yuhendra,

Department of Informatics, Faculty of Engineering,

Padang Institute of Technology,

Gajah Mada Kandis Nanggalo, Padang-West Sumatra, Indonesia.

Email: yuhendra@ieee.org

1. INTRODUCTION

Renewable energy refers to the energy derived from sources that are naturally replenished by nature like the sunlight for solar energy, the wind that powers turbines, the water for hydroelectric energy, and geothermal heat. These forms of energy generation are widely accepted as being vital for the continuance of life on planet earth [1, 2]. As the world's population grows larger, the energy requirements also increase. There was a 50% increase in human energy consumption from 1980-2003, which was caused by a growth of 42% in the global population, especially in developing countries. From this fact, it can be estimated that the demand for energy will increase by 57% by 2025. Indonesia is a country with the potential to generate large amounts of geothermal energy because it is located in the ring of fire and there are numerous active volcanoes on the tectonic plate that runs from Sumatra to Java, and from Bali and Maluku up to Sangeihe islands. Being located near volcanoes provides high enthalpy values in terms of the geothermal energy potential.

The geothermal resource refers to the amount of geothermal heat that can be generated if specific technological and economic conditions are met [3]. The Indonesian government stated at the 2000 World Geothermal congress that there were 276 locations that could be used for geothermal energy production. The locations were in Sumatra, Java, Bali, Kalimantan, Nusa Tenggara, Maluku, Sulawesi, Halmahera and Papua, and they estimated that the total potential energy that could be produced was 27.354 MWe (Mega Watt equivalent). More recent estimates of the geothermal potential are closer to 30.000 MWe. However, at present only 196 MW is generated, which represents around 40% of the total potential.

Satellite remote sensing (RS) offers a wide variety of image data with different characteristics like temporal, spatial, radiometric and spectral resolution. These features are useful because they match the requirements for monitoring environmental conditions and natural resources [3, 4]. Nowadays, large amounts of data are provided by satellite sensors like Landsat, IKONOS, SPOT-5, WorldView-2, QuickBird, GeoEye, and Orbview. In geological application, RS satellite images assist in conducting cost-effective geothermal exploration and in identifying the geothermal potential by ascertaining the land surface temperature (LST) through thermal infrared remote sensing (TIR). Now that more emphasis and resources are directed towards the search for renewable energy sources, TIR is regarded as vital when exploring geothermal resources [5]. One of the satellite sensors that TIR images can be obtained from is Landsat's Thermal Infrared Sensor (TIRS), which contains a wealth of information about the surface characteristics of the earth over the past 40 years. In particular, the thermal emission in band number ten on the sensor (10.60–11.19 μm) shows the changes in temperature observation capabilities. The images help to determine the thermal characteristics of an area and to detect temperature anomalies. The anomalies that indicate a high potential of geothermal resources are the areas with a high LST. TIR is acknowledged as an effective method for obtaining quantitative and qualitative LST data on regional and global scales [5, 6], and LST is regarded as a key factor in the study of geological surface activity [7]. Landsat TIR data can be used for monitoring environmental conditions, spatial decision making and monitoring water consumption. Also, it can be used for investigating urban microclimates, mapping sensible heat flux, monitoring volcanoes, and observing fire depleted flora by using burnt area mapping. Observing LST provides vital data on the climate and physical characteristics of the planet's surface. This information is used in studies on global warming, evapotranspiration, hydrological cycles, vegetation monitoring, urban climatic conditions, and the urban heat island effect [8]. LST is becoming more important in environmental studies and different methodologies are being implemented to observe LST from space [9]. LST is also mentioned in a number of studies on ecology, hydrology, and global change [10, 11].

LST specifically refers to the temperature of the Earth's surface, and it is obtained from either satellite imagery or by taking direct measurements. Satellite imagery helps to monitor the variation in the earth's resources and to observe the physical processes of surface energy and water balance at a local and global scale. There are several algorithms for estimating LST from satellite TIR measurements which are based on varying assumptions [12, 13]. The resulting LST measurements are crucial for evaporation modelling, climate modelling, and radiative transfer modelling [14].

This research analyses the land surface temperature to identify potential geothermal resources based on remote sensing using Landsat 8 TIRS imagery from satellite data. Since it was provided thermal infrared bands (Band 10 and 11) for estimating brightness surface. Single channel/Mono-window algorithms were used to generate the LST maps. And data set was combined with a digital elevation model (DEM) to identify the potential geothermal energy based on the variation in surface temperature. TIR remote sensing is an excellent method for obtaining LST data because the sensor detects most of the energy that emits from the surface of the land [15, 16].

2. RESEARCH METHOD

The research area in this case study is located West Sumatra in Indonesia with the geographic coordinates of 1°00'S 100°30'E. The majority of West Sumatra consists of the highlands of the Bukit Barisan mountain range which runs through the centre of the province from north to south. There are lowland areas surrounding the mountains and the west coast of the province faces the Indian Ocean. West Sumatra borders the provinces of North Sumatra and Riau in the north, as well as Jambi and Bengkulu to the south. This research focuses on the potential in 5 districts of West Sumatra, they are Pasaman, Agam, Solok, Tanah Datar, and Lima Puluh Kota as shown in Figure 1.

Landsat 8 carries two instruments: the first is TIRS (thermal infrared sensor) which includes band 10 and 11 and OLI (operational land imager) sensor Band (1-9), as shown in Table 1. The instruments collect image data from nine shortwave spectral bands (OLI1~ OLI9) over a 185 km swath with a 30 m spatial resolution for all bands except for the 15 m panchromatic band (OLI8); TIRS provides image data for both thermal bands (TIRS10, TIRS11) with a resolution of 100 m. The data for this study was taken on 01 July 2015

from Landsat 8 in a scene1 (path 127, row 60) and scene 2 (path 127, row 61). Panchromatic band 8 had a spatial resolution of 15 m. Universal Transverse Mercator (UTM) projection with zone 43 North and WGS84 datum were used for the datasets. Landsat TIR data can be used for observing water consumption, environmental conditions, and spatial decision-making. This type of data is also useful for examining microclimates in urban areas, mapping sensible heat flux, observing volcanoes, and monitoring fire damaged flora through burnt area mapping [17]. Tables and figures are presented center, as shown below and cited in the manuscript. Mono window algorithm used in this research to examine land surface temperature with Landsat-8 OLI imagery involved seven stages: pre-processing (Landsat-8 OLI imagery, cloud removal, ortho-rectification and mosaicking, colour balancing), and processing (processing temperature, extraction land surface temperature, top of atmosphere (ToA) spectral radiance, brightness temperature, estimation of emissivity, calculation NDVI and land surface temperature estimation), see in Figure 2.



Figure 1. Location of study area map in West Sumatra

Table 1. The Spectral range and spatial resolution of the Landsat 8 OLI and TIRS bands [18]

Sensor	Band	Spectral Range (μm)	Spatial Resolution (m)
OLI	1	0.43–0.45	30
	2	0.45–0.51	30
	3	0.53–0.59	30
	4	0.64–0.67	30
	5	0.85–0.88	30
	6	1.57–1.65	30
	7	2.11–2.29	20
	8	0.50–0.68	15
	9	1.36–1.38	30
TIRS	10	10.60–11.19	100
	11	11.50–12.51	100

2.1. Pre-processing of Landsat-8 OLI imagery

The Landsat-8 OLI images were in tagged image file format (TIFF) and the data type was integer. During image pre-processing, cloud removal is a common practice because areas that are of interest are sometimes obscured by clouds, which can make the land difficult or impossible to see. Cloud cover affects the view of the ground and causes problems when using a normalized difference vegetation index (NDVI), which in turn hinders the estimation of LST.

2.2. Ortho-rectification and mosaicking

Ortho-rectification is a process that removes the geometric distortions introduced during image capture and produces an image product that has planimetric geometry in order to precisely register to a ground coordinate system and the image scale. After computing geometric models, the final step is to generate ortho-rectified strips using a digital elevation model (DEM) and then to mosaic them into a colour-balanced image. The information about DEM is also discussed.

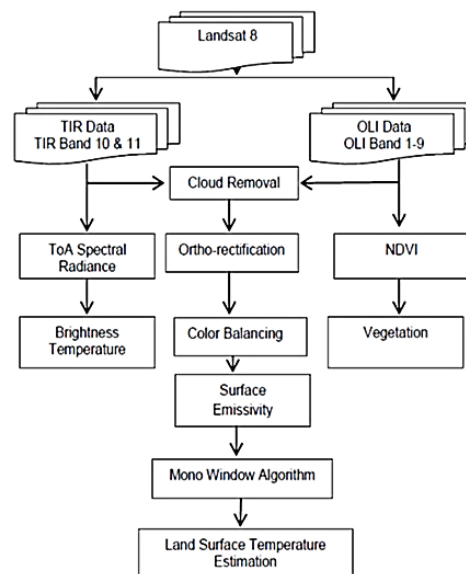


Figure 2. Mono window algorithm used to retrieve LST from Landsat 8 imagery

2.3. Processing temperature

Identification of heat anomalies can be performed using analysis of surface temperature according to the natural appearance. The Landsat 8 satellite has two sensors, the operational land imager (OLI) sensor and thermal infrared sensor (TIRS) sensor with 11 bands. The TIRS sensor provides two thermal bands which provide better signal-to-noise (SNR) radiometric performance quantised over a 12-bit dynamic range [17]. The OLI sensor contains 9 bands (1-9) and the TIRS sensors have 2 bands (10 and 11). The thermal bands (10 and 11) are vital for detecting and analysing the contrasts in land surface temperatures with 100 m spatial resolution.

2.4. Extraction land surface temperature

The following procedure and formula were used to identify the surface temperature, generate the temperature colour map and analyse the data. The thermal band (10.6-11.2 μm) (band 10) of the landsat 8 (OLI) sensor derived the LST of the study area, and the following formula was used to calculate the spectral radiance from the digital numbers (DN). The spectral radiance ($L\lambda$) is calculated with the equation [18].

2.5. Top of atmosphere (ToA) spectral radiance

Digital numbers (DN) of bands 1-9 were converted to top of atmosphere (ToA) and the spectral radiance ($L\lambda$) was calculated by multiplying multiplicative radiometric rescaling factor of the TIR bands with its corresponding TIR band and by adding an additive rescaling factor using (1). These results are then compared to DNs reported by the sensor to provide a set of bias and gains (radiometric calibration coefficients) for the sensor spectral bands.

$$L_{\lambda} = M_L \times Q_{cal} + A_L \quad (1)$$

where L_{λ} is the spectral radiance in watts/(m²srad⁻¹ μm⁻¹); M_L the band-specific multiplicative rescaling factor obtained from the metadata (0.000342); A_L is the band-specific additive rescaling factor obtained from the metadata (0.1); Q_{cal} is the DN value for the quantized and calibrated standard product pixel of band 10.

2.6. Brightness temperature (BT)

BT refers to the amount of electromagnetic radiation that travels upwards from the top of the atmosphere [19]. Thermal calibration involves converting the thermal DN values of the raw thermal bands from the TIR sensor into TOA spectral radiance, followed by the BT equation shown in (2),

$$T_{Landsat} = \frac{K_2}{\ln\left(\frac{K_1 \cdot \varepsilon}{L_{\lambda}} + 1\right)} - 273 \quad (2)$$

where: $T_{Landsat}$ Effective temperature (Celsius), L_{λ} Spectral radiance watt/(m²*srad*μm), K_1 , K_2 Calibration constants, ε emissivity value given when NDVI process yet.

2.7. Estimation of emissivity

Emissivity refers to the radioactive properties of an object and summarises its ability to emit radiation [20, 21]. To obtain the LST it is necessary to measure land surface emissivity. For this research, the emissivity of the land surface was obtained using NDVI as suggested by Zhang [22]. The corresponding land emissivity values as shown in Table 2 were then calculated from the NDVI results shown in (3).

Table 2. Estimation of land surface temperature from NDVI [22]

NDVI	Land surface emissivity (ε_i)
NDVI < -0.185	0.995
-0.185 ≤ NDVI < 0.157	0.970
0.157 ≤ NDVI ≤ 0.727	1.0094 + 0.0047 * Ln(NDVI)
NDVI > 0.727	0.990

The formula emissivity value given when NDVI process yet:

$$\varepsilon = 0.004 P_V + 0.986 \quad (3)$$

$$P_V = \left(\frac{NDVI - NDVI_{min}}{NDVI_{max} - NDVI_{min}} \right)^2 \quad (4)$$

2.8. Calculation NDVI

NDVI is a straightforward graphical indicator that analyses remote sensing measurements and assesses whether or not an area contains green vegetation. Studies show that NDVI provides accurate estimations of surface radiant temperatures [23-26]. NDVI is one of the outputs that was entered into the model to retrieve LST by using (5):

$$NDVI = \frac{NIR - R}{NIR + R} \quad (5)$$

where NIR is Near Infra-red band and R is the red band.

2.9. Land surface temperature (LST)

LST must be known in order to estimate LST, since it's a proportionality factor that scales blackbody radiance Planck's law (ρ) to predict emitted radiance, and it is the efficiency of transmitting thermal energy across the surface into the atmosphere [27]. The last step of retrieving the LST or the emissivity corrected land surface temperature (celsius) described computed as follows [27]:

$$T_{(Celsius)} = T_{(Kelvin)} - 272.15 \quad (6)$$

$$LST = \frac{T}{(1+w*\left(\frac{T}{\rho}\right)*\ln(e))} \quad (7)$$

where, w = wavelength, $\rho = 1.438*10^{-2}$ mK

3. RESULTS AND ANALYSIS

3.1. Colour balancing

The Landsat 8 image satellite images have been processed into red (R), green (G), and blue (B) colour composites (balancing) with a spatial resolution of 15 m. A color composite of RGB were used as basis of visual interpretation. Figure 3 (a) shows the colour combinations. The RGB 432 band (natural colour) denotes natural object like vegetation since the colour is green, while RGB 5, 6, 7 showed false color. Both composites were used for volcanic products and lineament analyses. And also, to establish the density level of vegetation, the red image is useful to gather information about the size of the forest and the maturity of the vegetation as shown in Figure 3 (b) covers for estimating the leaf condition related to geothermal system beneath the surface.

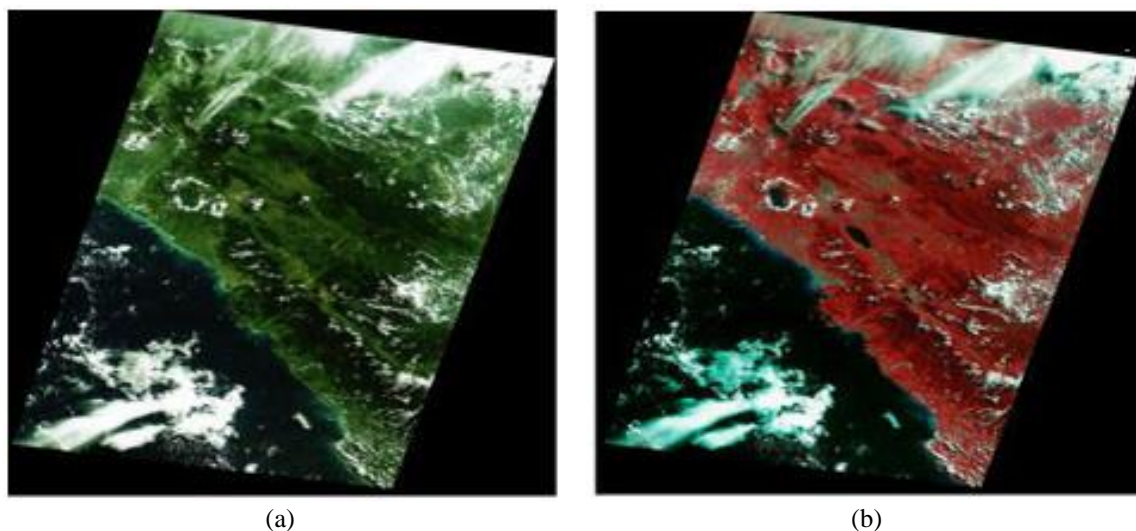


Figure 3. West Sumatra area image processing with colour balancing; (a) RGB band 432, (b) RGB band 567

3.2. SRTM DEM and countour

Various types of data like shuttle radar topography mission (SRTM) data and digital elevation model (DEM) data were used to prepare LST maps of the area. The DEM was derived from topographical maps, and the geographical coordinate system and WGS 84 datum were used to perform single map rectification. The geo-referenced topographical maps of the area were mosaic. The original SRTM DEM was used for the contouring procedure. SRTM data requires a lot of pre-processing to make sure there are no spurious artefacts which could become problematic during the analysis, for example, pits, spikes, and patches of no data. The final map represents the digital elevation model for all of West Sumatra with 30 m spatial resolution as shown in Figure 4. Based on Figure 4 derived from SRTM, some parts of West Sumatra are located directly on or extremely close to active volcanoes (Talang, Merapi, Singalong, Sago). Figure 5 shows the contour characteristics which were derived from the DEM data. Contours connect points with equal values like elevation, temperatures, precipitation, pollution, and atmospheric pressure. The distribution of polylines in the contours represent the variation in values over a surface area.

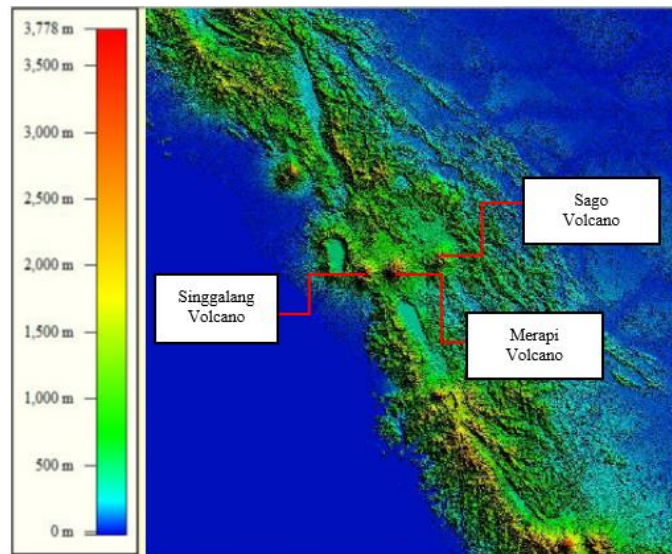


Figure 4. SRTM DEM with spatial resolution 30 m

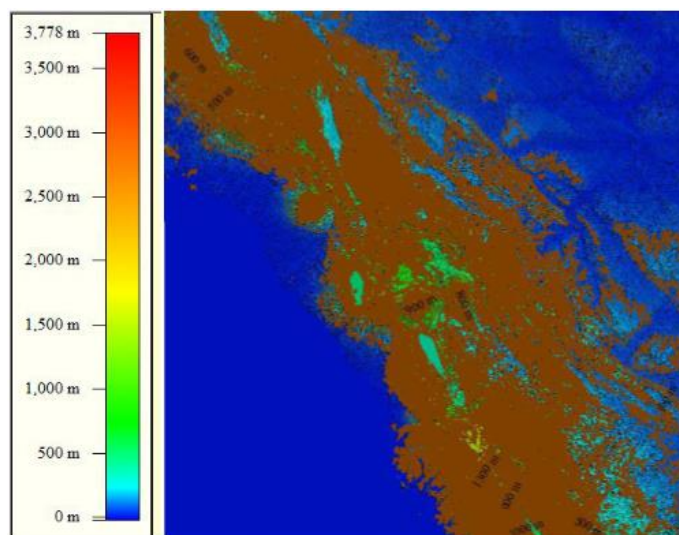
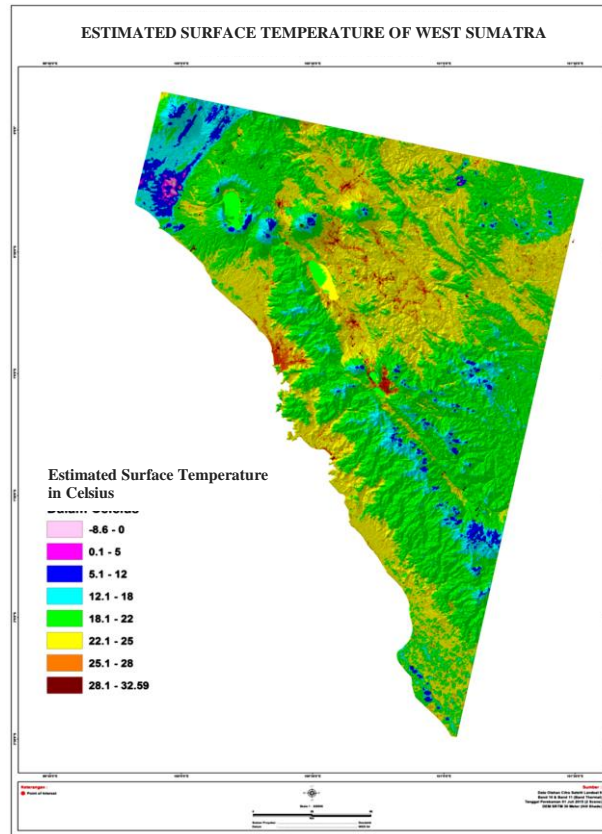


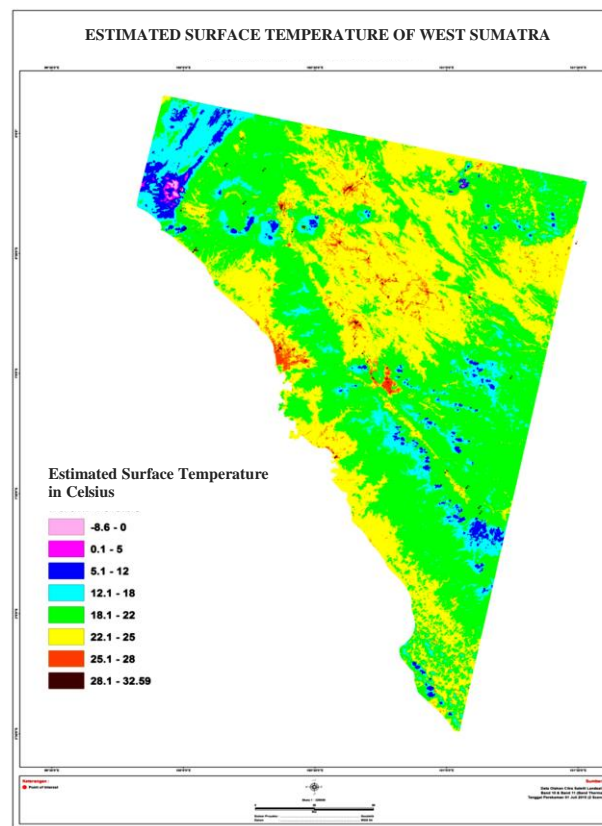
Figure 5. Contour characteristics derived from DEM SRTM

Air temperature decreases when ascending through the troposphere and into the high atmosphere. The rate of lapse shows that the temperature falls by $0.65^{\circ}\text{C}/100$ meters. The fall in temperature at higher altitudes is because the earth's surface acts as an energy source that heats the air and makes the temperature higher on the planet's surface. The land surface temperature estimates that were derived from the satellite imagery indicate patches of high and low temperatures, as shown in Figures 6 (a) and 6 (b).

The calculated land surface temperature as shown in Figures 6 (a) and (b) that in West Sumatra, the temperature ranged from -8.6°C to 32.59°C , which is represented by graduated pink to brown shading. The areas that were predicted to be higher in temperature are clearly identified (brown colour pixels) in the dataset. The Lima Pulu Kota, Tanah Datar, Solok and South Solok city areas show high-temperature values (Brown) ranging from 28.1°C to 32.59°C because of their high thermal influencing properties. Temperatures were lower (Pink) in the north-east region and the range distribution was from -8.6°C to 5°C . The hill-shade function as shown in Figures 6 (a) and 7 (a) provides the hypothetical illumination of a surface by establishing a value for each of the cells contained in a raster. By working out the illumination value of each of the cells and setting a hypothetical light source, visualisation of surfaces can be enhanced for analysis or graphical display. In Figure 7, show the NDVI also used to identify the vegetation covers for estimating the leaf condition related to geothermal system beneath the surface manifestation.

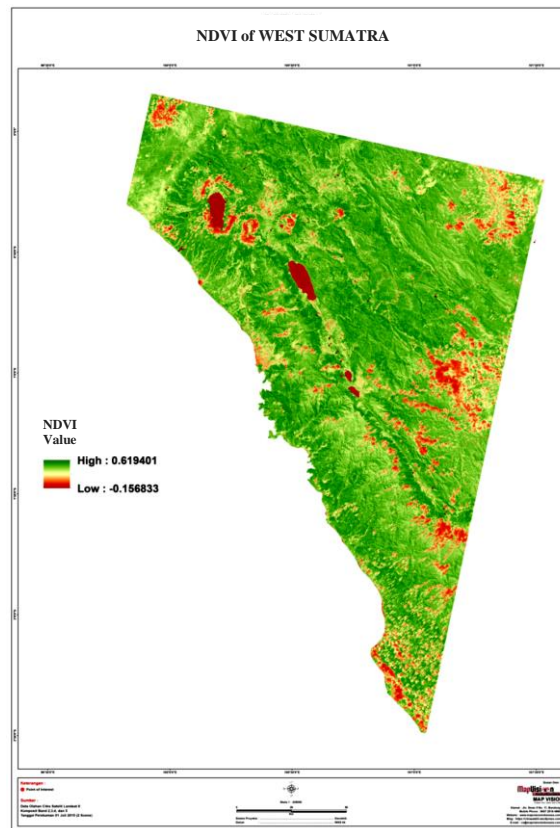


(a)

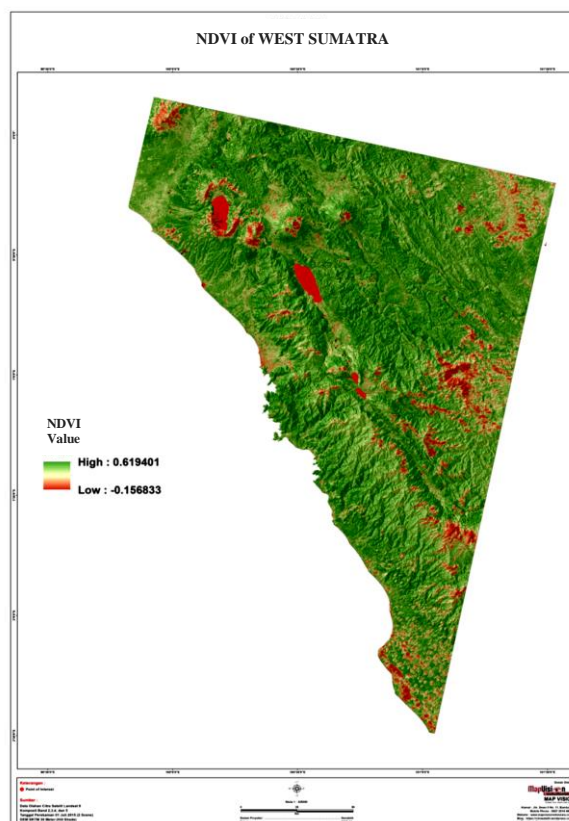


(b)

Figure 6. (a) Map of LST derived with DEM SRTM 30 m hill-shade, (b) without hill-shade



(a)



(b)

Figure 7. (a) Map of NDVI Overlay DEM SRTM 30 m hill-shade (band 2, 3, 4, 5), (b) without hill-shade

4. CONCLUSION

The thermal imagery from Landsat-8 OLI/TIRS bands can be used to detect surface temperature, which in turn allows for the identification of geothermal energy potential depend on surface parameters temperature, emissivity and also atmospheric correction. From this method, the brightness temperature was derive from LST map of West Sumatra shows that ranged from -8.6 C^0 to 32.59 C^0 and the different temperatures are represented. The identification area from calculated result clearly identifies the hot areas in the dataset such as Lima Puluh Kota, Tanah Datar, Solok, and South Solok areas showed the high-temperature value in the range of 28.1 C^0 to 32.59 C^0 which means that they possess high potential for generating thermal energy. The possibility of accurately and efficiently approach to geothermal area detection combining with geological survey analysis was consideration for future research.

ACKNOWLEDGEMENTS

The authors would like to offer thanks to the Directorate of Higher Education (DIKTI) for the research funding, the US Geological Survey (USGS) who provided free Landsat-8 imagery data, and Map Vision for the data processing. Also, gratitude is expressed to the anonymous reviewers for their invaluable comments and suggestions which improved the clarity and quality of the study.

REFERENCES

- [1] Singh H. K., "Geothermal energy potential of Indian oilfields," *Geomech. Geophys. Geo-energ. Geo-resour.*, vol. 6, no. 19, pp. 1-9, 2020.
- [2] Ramachandra T. V., "Solar energy potential assessment using GIS," *Energy Education Science and Technology*, vol. 18, no. 2, pp. 101-114, 2007.
- [3] Yuhendra, Joshapat T. S., "Assessment of multi temporal image fusion for remote sensing application," *International Journal on advance science engineering information technology*, vol. 7, no. 3, pp. 778-784, 2017.
- [4] Yuhendra, Joshapat T. S., "A Quality of images fusion for remote sensing applications," *TELKOMNIKA Telecommunication, Computing, Electronics and Control*, vol. 14, no. 1, pp. 378-386, 2016.
- [5] Qin Q., Zhang N., Nan P., Chai L., "Geothermal area detection using Landsat ETM+ thermal infrared data and its mechanistic analysis-A case study in Tengchong, China," *International Journal of Applied Earth Observation and Geo-information*, vol. 13, pp. 552-559, 2011.
- [6] Zhang Z., He G., Wang M., Long T., Wang G., Zhang X., Jiao W., "Towards an operational method for land surface temperature retrieval from Landsat 8 data," *Remote Sensing Letter*, vol. 7, no. 3, pp. 279-288, 2016.
- [7] Mujabar S., Rao V., "Estimation and analysis of land surface temperature of Jubail Industrial City, Saudi Arabia, by using remote sensing and GIS technologies," *Arab J Geosci*, vol. 11, no. 742, pp.1-13, 2018.
- [8] Sahana M., Ahmed R. & Sajjad H., "Analyzing land surface temperature distribution in response to land use/land cover change using split window algorithm and spectral radiance model in Sundarban Biosphere Reserve, India," *Model. Earth Syst. Environ*, vol. 2, no. 81, pp. 1-11, 2016.
- [9] Li Z. L., Tang B. H., Wu H., Ren H., Yan G., Wan Z., Trigo I. F., Sobrino J. A., "Satellite-derived land surface temperature: current status and perspectives," *Remote Sensing Environment*, vol. 131, pp. 14-37, 2013.
- [10] Yu X., Guo X., Wu Z., "Land surface temperature retrieval from Landsat 8 TIRS comparison between radiative transfer equation based method, split window algorithm and single channel method," *Remote Sensing*, vol. 6, pp. 9829-9852, 2016.
- [11] Liang S., Li X., Wang J., "Advanced remote sensing: Terrestrial information extraction and applications," *Academic Press*, 2012.
- [12] Zhang Z., He G., "Generation of Landsat surface temperature product for China, 2000–2010," *Int. J. Remote Sens.*, vol. 34, pp. 7369-7375, 2013.
- [13] Li Z., Tang B., Wu H., et al., "Satellite-derived land surface temperature: Current status and perspectives," *Remote Sensing of Environment*, vol. 131, pp. 14-37, 2013.
- [14] Xiaolei Yu, Xulin Guo, and Zhaocong Wu, "Land surface temperature retrieval from landsat 8 TIRS—comparison between radiative transfer equation-based method, split window algorithm and single channel method," *Remote Sensing*, vol. 6, no. 10, pp. 9829-9852, 2014.
- [15] Du C., Ren H., Qin Q., Meng J., and Zhao S., "A practical split-window algorithm for estimating land surface temperature from Landsat 8 data," *Remote Sensing*, vol. 7, no. 1, pp. 647-665, 2015.
- [16] Jin M., Li J., Wang C., and Shang R., "A Practical Split window algorithm for retrieving land surface temperature from landsat-8 Data and a case study of an urban area in China," *Remote Sensing*, vol. 7, no. 4, pp. 647-65, 2015.
- [17] Wang F., Qin Z., Song C., Tu L., Karnieli A., Zhao S., "An improved mono-window algorithm for land surface temperature retrieval from landsat 8 thermal infrared sensor data," *Remote Sensing*, vol. 7, no. 4, pp. 4268-4289, 2015.
- [18] Wang S., He L., and Hu W., "A temperature and emissivity separation algorithm for landsat-8 thermal infrared sensor data," *Remote Sensing*, vol. 7, no. 8, pp. 9904-9927, 2015.
- [19] Maimaitiyiming M., Ghulm A., Tiyip T., Pla F., Carmona P. L., Halik U., Sawut M., Caetano M., "Effect of green space spatial pattern on the land surface temperature: Implications for sustainable urban planning and climate change adaptation," *ISPRS Journal of Photogrammetry and Remote Sensing*, vol. 89, pp. 59-66, 2014.

- [20] Jimenez-Munoz J. C., Sobrino J. A., "Split-window coefficients for land surface temperature retrieval from low-resolution thermal infrared sensors," *IEEE Geoscience. Remote Sens. Letter*, vol. 5, pp. 806–809, 2008.
- [21] Solanky V., Singh S., Katiyar S. K., "Land Surface Temperature Estimation Using Remote Sensing Data," *Hydrologic Modeling*, pp.343-351, 2018.
- [22] Boori M., S. Balzter H., Choudhary K., Kovelskiy V., "A Comparison of land surface temperature derived from AMSR-2, Landsat and Aster satellite data," *Journal of Geography and Geology*, vol. 7, no. 3, pp. 985-988, 2015.
- [23] Zhang Y., "Land surface temperature retrieval from CBERS-02 IRMSS thermal infrared data and its applications in quantitative analysis of urban heat island effect," *Journal of Remote Sensing*, vol. 10, pp.789-797, 2006.
- [24] Guha S., Govil H., Dey A., Gill N., "Analytical study of land surface temperature with NDVI and NDBI using Landsat 8 OLI and TIRS data in Florence and Naples city, Italy," *European Journal of Remote Sensing*, vol. 51, no. 1, pp. 667-678, 2018.
- [25] Balew A., Korme T., "Monitoring land surface temperature in Bahir Dar city and its surrounding using Landsat images," *Egyptian Journal of Remote Sensing and Space Science*, pp. 1-16, 2020.
- [26] Alemu M. M., "Analysis of Spatio-temporal Land Surface Temperature and Normalized Difference Vegetation Index Changes in the Andassa Watershed, Blue Nile Basin, Ethiopia," *Journal of Resources and Ecology*, vol. 10, no. 1, pp. 77-85, 2019.
- [27] Avdan U., Jovanovska G., "Algorithm for Automated Mapping of Land Surface Temperature Using LANDSAT 8 Satellite Data," *Journal of Sensors*, vol. 2016, no. 2, pp. 1-8, 2016.

BIOGRAPHIES OF AUTHORS



Yuhendra was born in Riau Island, Indonesia, in 1970. He received the bachelor degree in Electrical Engineering from Padang Institute of Technology, Indonesia in 1997, and master degree in Computer System and Informatics from Gadjah Mada University, Indonesia, in 1998. Hold in Doctoral degree in Graduated Advance Integration of Science, Chiba University, Japan. He became member of IAENG No.127201 since 2014. In 2003, he joined the Department of Electrical Engineering, Faculty of Industrial Engineering, as a Lecture. His current research interest includes; artificial intelligence, image processing, GIS, remote sensing with research group Image Processing and Artificial Intelligence (i-PAi).



Josaphat Tetuko Sri Sumantyo was born in Bandung, Indonesia, in 1970. He received the B.Eng. and M.Eng. degrees in electrical and computer engineering from Kanazawa University, Kanazawa, Japan, in 1995 and 1997, respectively, and the Ph.D. degree in artificial system sciences from Chiba University, Chiba, Japan, in 2002. From 2002 to 2005, he was a Lecturer with the Center for Frontier Electronics and Photonics, Chiba University, Japan. From 2005 to 2013, he was an Associate Professor with the Center for Environmental Remote Sensing, Chiba University, where he is currently a Full Professor. His research interests include theoretically scattering microwave analysis and its applications in microwave (radar) remote sensing, especially synthetic aperture radar and subsurface radar (VLF), including DInSAR and PS-InSAR, analysis and design of antennas for mobile satellite communications and microwave sensors, development of microwave sensors, including SAR for unmanned aerial vehicle and microsatellite development